

# C-O Bond Scission during Methanol Decomposition on (1×1)Pt(110)

Jianhua Wang and R. I. Masel\*

Contribution from the University of Illinois, 1209 West California Street, Urbana, Illinois 61801.  
Received August 23, 1990

**Abstract:** Recently there has been some controversy whether C-O bond scission occurs during methanol decomposition on the (111) faces of platinum and palladium. Here, the decomposition of methanol on Pt(110) is examined by TPD and EELS. It is found that, on the (1×1) reconstruction of Pt(110), the methanol adsorbs molecularly at 100 K. When the layer is heated to 140 K, the C-O bond breaks to yield water and a mixture of CH<sub>x,ad</sub> species. The CH<sub>x,ad</sub> species then further react to form CH<sub>4</sub>, H<sub>ad</sub>, C<sub>ad</sub>, and some as yet unidentified higher hydrocarbons. By comparison, if the sample preparation procedure is changed to produce a (2×1) reconstruction no water, methane, carbon, or higher hydrocarbons are detected. These results demonstrate that C-O bond scission can occur during methanol decomposition on platinum. However, the extent of bond scission is strongly affected by small changes in the sample preparation procedures and surface structure of the sample. This may explain why the previous observations of C-O bond scission from some laboratories were not reproduced in other laboratories.

## Introduction

Recently, there has been some controversy whether C-O bond scission occurs during methanol decomposition on platinum and palladium. Levis et al.<sup>1</sup> examined methanol decomposition on Pd(111) with XPS and SIMS. They found that some of the C-O bonds in the methanol broke upon heating to yield adsorbed CH<sub>3</sub> groups. However, Guo et al.<sup>2</sup> examined the same reaction on a different Pd(111) sample with TPD. Guo did not detect any of the products that one would expect if the C-O bond broke. Guo also did not detect any isotope exchange between the CO groups in <sup>12</sup>CH<sub>3</sub><sup>16</sup>OH and <sup>13</sup>CH<sub>3</sub><sup>18</sup>OH. As a result, Guo et al. concluded that their Pd(111) sample does not catalyze the scission of the C-O bond in methanol.

The situation is as confusing with platinum. Levis et al.<sup>3</sup> examined methanol decomposition on Pt(111) with SIMS. They found that, as with Pd(111), some of the C-O bonds break upon heating to yield adsorbed CH<sub>3</sub> groups. In unpublished work, Abbas and Madix<sup>4</sup> have detected C-O bond scission on Pt(111) as evidenced by carbon deposition on their clean samples and methane formation when their samples were poisoned with sulfur. However, Sexton<sup>5</sup> and Gibson et al.<sup>29</sup> did not detect C-O bond scission on Pt(111) under similar conditions. Attard et al.<sup>22</sup> did not detect C-O bond scission during methanol decomposition on (2×1)Pt(110). Thus, it seems that there are some differences in the results of the various experiments which need to be explained.

The objective of this paper is to see if changes in the surface structure of the catalyst would have an important influence on the rate of C-O bond scission. We choose to examine methanol decomposition on (1×1)Pt(110). (1×1)Pt(110) has quite a different surface structure than Pt(111) (see Figure 1). In previous work, we found that (1×1)Pt(110) is unusually active for the scission of carbon-carbon single bonds.<sup>6</sup> Carbon-carbon and carbon-oxygen bond scission processes often show similar structural sensitivities. Thus, there is reason to suspect that (1×1)Pt(110) might also be active for the scission of carbon-oxygen single bonds. In a previous paper,<sup>7</sup> we presented some TPD data which suggests that carbon-oxygen bond scission can occur during methanol decomposition on (1×1)Pt(110). No C-O bond scission was detected on (2×1)Pt(110). The objective of this paper is to examine the decomposition of methanol with TPD, AES, and EELS to clarify the mechanism of methanol decomposition on (1×1)Pt(110) and in particular to see if the chemistry observed by Levis et al. does occur on (1×1)Pt(110).

## Experimental Section

The experiments were done using the apparatus and procedures described previously.<sup>7-9</sup> A Pt(110) single crystal sample was cut from a

Metron single crystal rod. The sample was polished with diamond paste and then mounted in one of two vacuum systems. The sample was then oxidized, sputtered, and annealed until no impurities could be detected by AES. A sharp (2×1) LEED pattern was seen at this stage. Next the sample was converted to a (1×1) reconstruction via a procedure similar to that of Bonzel et al.<sup>10</sup> The sample was heated to 600 K, exposed to 1 × 10<sup>-7</sup> Torr of CO, and then slowly cooled to 250 K in 1 × 10<sup>-7</sup> Torr of CO. This procedure produced a CO-covered Pt(110) sample with a well-developed (2×1)plg1 LEED structure and relatively high intensity between the LEED spots. The CO was then pumped away, and the sample was cooled to 100 K. The sample was then bombarded for 3 min with 100 V electrons at an average current of 3 mA/cm<sup>2</sup> to desorb the CO remaining on the surface. The sample temperature rose to 200-220 K during the electron-bombardment process. A trace of some sort of carbonaceous deposit was left behind on the crystal at the end of the electron-bombardment procedure. This carbonaceous deposit was removed by exposing the sample to 1 × 10<sup>-7</sup> Torr of hydrogen at 200 K for 4 min. Then the hydrogen was removed by bombarding the surface with electrons for another 40 s at 90-170 K. At the end of this treatment the sample showed a sharp (1×1) LEED pattern with little intensity between the spots. The sample also appeared clean by AES. However, TPD and EELS revealed that there was still a small amount of residual CO, H<sub>2</sub>, and adsorbed carbon on the surface. Occasionally, there was also some subsurface oxygen.

There was some concern that these small amounts of impurities might be responsible for some of the novel chemistry discussed below. As a result, we also created an "almost (2×1)Pt(110)" surface by preparing a (1×1)Pt(110) sample as above and then annealing to 400 or 500 K to partially convert the sample back to a (2×1) reconstruction. The sample was unchanged upon annealing to 300 K. The sample still showed a (1×1) LEED pattern after a brief anneal at 400 K. However, the (1×1) pattern was no longer sharp. Half-order spots were quite visible upon annealing to 500 K for 2 min. However, the half-order spots were not as sharp as with the (2×1)Pt(110) sample.

Once the sample was prepared, it was exposed to a measured amount of vacuum-distilled methanol through a capillary array doser. Doses were calibrated by comparing to background, and a separate coverage calibration was done with AES. Subsequently, the sample was examined with TPD, AES, and EELS.

(1) Levis, R. J.; Zhicheng, J.; Winograd, N. *J. Am. Chem. Soc.* **1988**, *110*, 4431; *J. Am. Chem. Soc.* **1989**, *111*, 4605.

(2) Guo, X.; Hanley, L.; Yates, J. T. *J. Am. Chem. Soc.* **1989**, *111*, 3155.

(3) Levis, R. J.; Zhicheng, J.; Winograd, N.; Akhter, S.; White, J. M. *Catal. Lett.* **1988**, *1*, 385.

(4) Abbas, N. M.; Madix, R. J. Unpublished work. Madix, R. J. Personal communication, 1990. See: Abbas, N. Ph.D. Dissertation, Stanford University, 1981.

(5) Sexton, B. A. *Surf. Sci.* **1981**, *102*, 271.

(6) Yagasaki, E.; Masel, R. I. *J. Am. Chem. Soc.* **1990**, *112*, 8746.

(7) Wang, J.; Masel, R. I. *J. Catal.* **1990**, *126*, 519.

(8) Yagasaki, E.; Backman, A. L.; Masel, R. I. *J. Phys. Chem.* **1990**, *94*, 1066.

(9) Yagasaki, E.; Masel, R. I. *Surf. Sci.* **1989**, *222*, 430.

(10) Ferrer, S.; Bonzel, H. P. *Surf. Sci.* **1982**, *119*, 234.

\* To whom correspondence should be addressed.

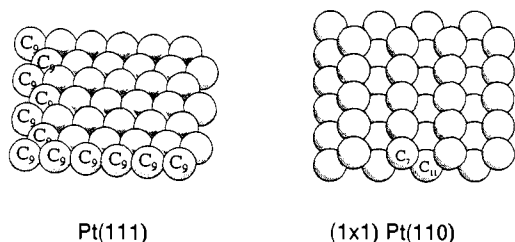


**Figure 1.** Comparison of the surface structures of Pt(111) and (1×1)-Pt(110).

The TPD work was done in the same apparatus used for our previous studies of ethylene adsorption on Pt(110).<sup>8</sup> The UHV system was of standard design with a working base pressure of  $1 \times 10^{-10}$  Torr. The system was equipped with a PHI 4-161 sputter gun, a PHI 15-120 LEED/AES system, and a Balzers QMA 112 mass spectrometer.

During a TPD run, the sample was cleaned until no impurities could be detected by AES and a (1×1) LEED pattern was seen. The sample was then dosed with a measured amount of vacuum-distilled methanol through a capillary array. The sample was rotated so it faced an opening in a shield over the mass spectrometer. The geometry was such that only the front face of the crystal was in line of sight with the mass spectrometer. Next, the sample was heated at a fixed rate of 14 K/s under computer control, and a TPD spectrum was recorded.

In separate runs, coverages were calibrated by comparison the AES spectrum of a monolayer of CO and that of 1 langmuir of methanol. Absolute coverages were estimated by comparing the ratio of the platinum peak at 237 eV to the carbon peak at 272 eV for the adsorbed CO and the adsorbed methanol.

The EELS work was done in a second apparatus. This apparatus consisted of a UHV system with a working base pressure of  $5 \times 10^{-11}$  Torr. The UHV system was equipped with a PHI 4-161 sputter gun, a PHI 15-120 LEED/AES unit, a Ribler QX mass spectrometer, and an LK Technologies LK-2000-DAC EELS spectrometer. During a EELS run, the sample was cleaned until no impurities could be detected by AES and a sharp (1×1) LEED pattern was seen. The sample was then exposed to methanol at 100 K and cooled to 92 K. An EELS spectrum was then recorded. Subsequent spectra were taken by sequentially annealing to a higher temperature for 1 min, cooling back to 92 K, and then recording an EELS spectrum. Generally, most of the measurements were done by sequentially heating the sample to progressively higher temperatures. However, key spectra were reproduced via nonsequential heating to insure that buildup of impurities from the background was not contributing to the results. The doser calibrations were somewhat uncertain during the EELS measurements. Hence, we used AES as our primary coverage calibration. The AES measurements did have a difficulty in that, at beam currents of 30–50  $\mu\text{A}$ , the layer degraded over a 30-min period. We ran most of our AES measurements with a beam current of 4–5  $\mu\text{A}$  and did all of our AES measurements quickly to avoid significant changes in the layer during the scan. We also did a few measurements at a beam current of 1  $\mu\text{A}$  to check for degradation of the layer when we are turning on the beam. (None was detected.) In this way, we believe that we were able to take AES data and yet avoid complications due to beam damage. All of the other experimental techniques were standard. One should refer to Backman<sup>11</sup> for more details.

## Results

Figure 2 shows a composite TPD spectrum for methanol decomposition on (1×1)Pt(110) from Wang et al.<sup>7</sup> Four species are seen during methanol decomposition on (1×1)Pt(110): methanol, water, methane, and hydrogen. The methanol desorbs in a single peak at 130 K. The water desorbs in a peak at 140 K and a tail extending up to 250 K independent of exposure. The methane desorbs in a single peak, which shifts from 260 to 245 K with increasing exposure. The hydrogen desorbs in a peak at 300 K and a second peak at 430 K. There is also a 2 amu peak at 130 K which appears to be associated with cracking of water and methanol in the ionizer of the mass spectrometer.

We also have detected a small CO peak during methanol TPD on (1×1)Pt(110). However, that peak appears to be associated with background CO since it does not grow significantly with increasing methanol exposure. (The CO background is high because CO is used to prepare the (1×1) reconstruction.) The

TPD spectra from methanol(1.0L) on (1×1)Pt(110)

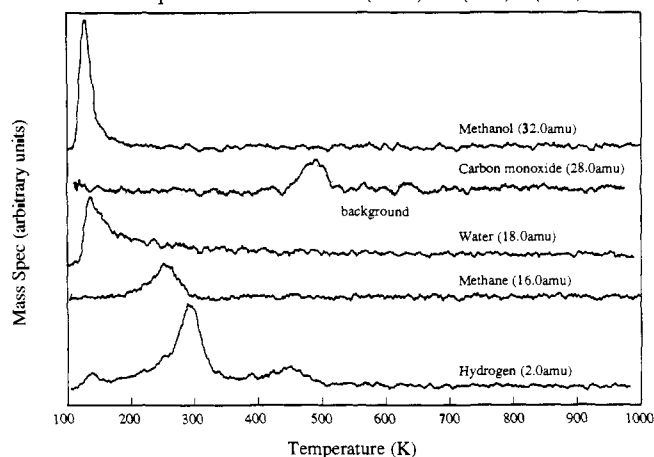


**Figure 2.** A series of TPD spectra taken by exposing a clean (1×1)Pt(110) sample to 1 langmuir of methanol and then heating at 24 K/s, from Wang and Masel.<sup>7</sup>

CO peak in Figure 2 corresponds to about 5% of a monolayer of CO.

An attempt was made to look for many other species during the TPD experiments. However, only methanol, methane, hydrogen, carbon monoxide, and water were detected.

Experiments were also done to examine the changes in the TPD spectra as the surface was converted from a (1×1) to a (2×1) reconstruction.<sup>6</sup> When a clean (1×1)Pt(110) surface is annealed at 300 K prior to exposure to methanol, the sample still shows a sharp (1×1) LEED pattern. The TPD spectrum from the annealed surface is identical to that from an unannealed surface. However, if the surface is annealed at 400 K prior to admission of the methanol, weak (2×1) spots are seen in LEED. Simultaneously, the methane and water peaks in TPD are attenuated by a factor of 5. By 500 K, no methane or water desorption can be detected. The CO peak grows by more than 1 order of magnitude, and a (2×1) pattern is seen in LEED. Hence, it seems that production of water and methane is unique to (1×1)Pt(110). No water or methane formation is observed on (2×1)Pt(110). Instead, the major products are CO and hydrogen.

The evolution of the TPD spectra with exposure has also been explored by Wang and Masel.<sup>7</sup> The hydrogen and methane peaks grow with increasing exposure and then saturate at about a 3-langmuir exposure. The coverage dependence of the 18 amu peak is more complex because methanol has a small cracking fraction at 18 amu corresponding to 2% of the water peak in Figure 2. This cracking fraction does make a small contribution to the 18 amu peak at methanol exposures above 6 langmuirs. As a result, the 18 amu peak does not ever quite saturate with increasing methanol coverage. Still, if the expected methanol cracking fraction is subtracted away from the measured 18 amu peak, the resultant peak does saturate at a 3–6-langmuir exposure.

Finally, the methanol peak shows complex behavior. At low exposures, no methanol desorption is detected. Instead all the methanol reacts upon heating. At exposures above 0.10 langmuir, methanol desorption is seen. Initially, the methanol desorbs in a broad peak at 130 K with a tail extending up to 190 K. However, at exposures above 0.6 L, the peak sharpens. At a 1-langmuir exposure, only a 130 K peak is seen. Our interpretation of this data is that the 130 K peak is associated with monolayer desorption. At moderate exposures, there also is a tail extending to 190 K associated with monolayer desorption. However, that tail disappears at higher exposures presumably because the methanol on the surface at 140 K decomposes before it desorbs.

Experiments were also done to look for reactions between the methanol and adsorbed hydrogen. Figure 3 shows a series of TPD spectra taken by preparing a (1×1)Pt(110) sample with deuterium rather than hydrogen, adsorbing 0.7 monolayers (2.21 langmuirs) of methanol, and, 10 langmuirs of deuterium, and then heating at 14 K/s. There are peaks at 130 K corresponding to water

(11) Backman, A. L. Ph.D. Dissertation, University of Illinois, 1990.

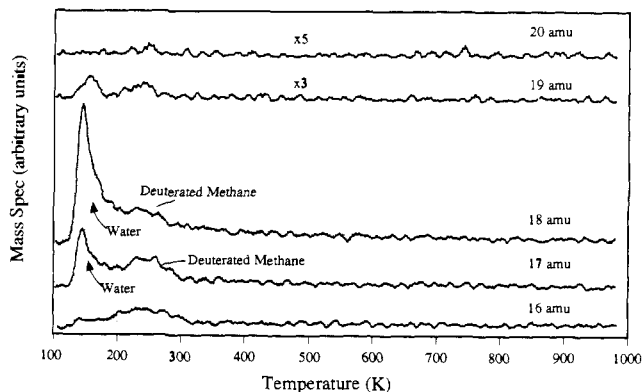


**Figure 3.** Solid line: a series of TPD spectra taken by preparing a  $(1 \times 1)\text{Pt}(110)$  sample with deuterium rather than hydrogen, exposing the surface to 2.21 langmuirs of methanol, 10 langmuirs of deuterium, and then heating at 14 K/s. Dotted lines: three copies of an 18 amu (water) spectrum measured in the absence of deuterium. The height of the dotted 18-amu spectrum has been adjusted to match the height of the water peak at 17 and 16 amu.

( $\text{H}_2\text{O}$ ) and monodeuterated water (HDO) desorption and a second group of peaks at 240 K corresponding to desorption of  $\text{CH}_4$ ,  $\text{CH}_3\text{D}$ ,  $\text{CH}_2\text{D}_2$ ,  $\text{CHD}_3$ , and  $\text{CD}_4$ . Note, however, that the 19 amu peak from deuterated water is more than 1 order of magnitude smaller than the 18 amu peak from undeuterated water. As a result, it appears that the water product is not substantially deuterated when methanol and deuterium are coadsorbed. In contrast, the methane product is clearly deuterated. There are large peaks at 240 K in the 16, 17, and 18 amu TPD spectra. The peak areas vary in a 1:1.7:1 ratio. The presence of the large 18 amu peak at 240 K implies that  $\text{CH}_2\text{D}_2$  forms when methanol and deuterium are coadsorbed. The 17 amu peak is harder to interpret, since it contains contributions from both  $\text{CH}_2\text{D}_2$  and  $\text{CH}_3\text{D}$ . However, the 17 amu peak in Figure 3 is larger than one would expect from  $\text{CH}_2\text{D}_2$ .<sup>18</sup> Thus, it appears that some  $\text{CH}_3\text{D}$  forms when methanol and deuterium are coadsorbed. The 16 amu peak is even more difficult to interpret. It happens that if one adds up the expected contribution at 16 amu from  $\text{CH}_2\text{D}_2$  and  $\text{CH}_3\text{D}$ , one can account for the whole 16 amu peak. Thus, it is unclear whether any  $\text{CH}_4$  forms. Certainly  $\text{CH}_4$  is not a major reaction product. Hence, it appears that when methanol and deuterium react on  $(1 \times 1)\text{Pt}(110)$ , the main carbon- and oxygen-containing products are  $\text{CH}_2\text{D}_2$ ,  $\text{CH}_3\text{D}$ , and  $\text{H}_2\text{O}$ .

EELS was used to clarify the details of the methanol decomposition process in the experiments described above. Figure 4 shows a series of EELS spectra taken by exposing a clean  $(2 \times 1)\text{Pt}(110)$  sample to nominally 0.4 langmuir of methanol and then annealing to successively higher temperatures. A 0.4-langmuir exposure was chosen for these experiments because the tail in the methanol TPD peak corresponding to desorption of methanol from the first monolayer was largest at an exposure of 0.2–0.4 langmuir. AES indicates that a nominal 0.4-langmuir exposure puts  $(3\text{--}4) \times 10^{14}$  molecules/ $\text{cm}^2$  on the surface.

The data in Figure 4 show that, at 100 K, there are distinct peaks at 740, 1060, 1135, 1470, 2960, and 3275  $\text{cm}^{-1}$ . The 3275  $\text{cm}^{-1}$  peak shifts to 3400  $\text{cm}^{-1}$  upon heating to 140 K, and the 1135  $\text{cm}^{-1}$  peak grows relative to the rest. However, there is little other change in the spectrum. Nevertheless, AES indicates that, with a 0.4-langmuir exposure, 10% of the methanol desorbs upon heating to 140 K. A small methanol peak is also seen in TPD. Apparently, however, the change in the methanol coverage upon heating to 140 K observed in TPD and AES does not produce a significant change in the intensity of the EELS peaks, as expected since the fractional change in coverage is small.

At 200 K the 760 and 3300  $\text{cm}^{-1}$  peaks disappear and all of the other peaks are attenuated. However, there is little change in the relative sizes of the other peaks. There is also a new peak at 2070  $\text{cm}^{-1}$ . The peak seems to grow during the EELS scan. Therefore, we assign the 2070  $\text{cm}^{-1}$  peak to buildup of background CO.

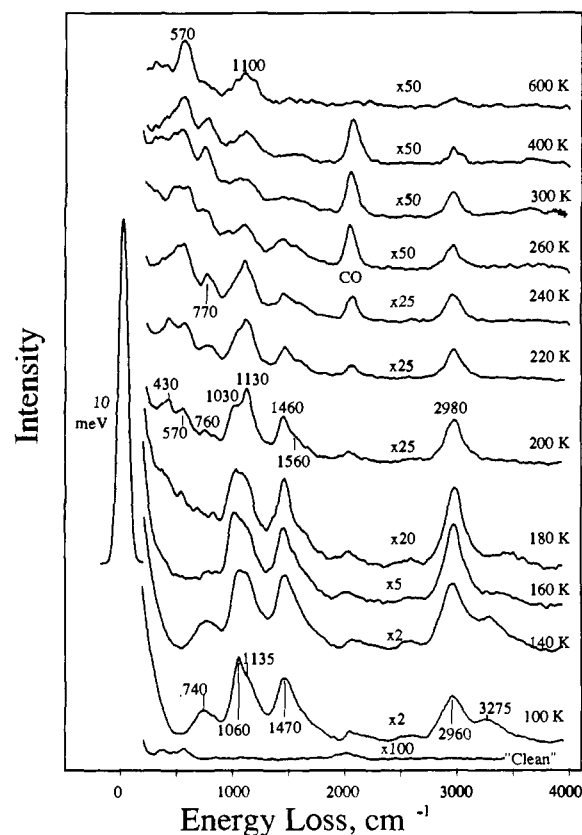


**Figure 4.** A series of EELS spectra taken by exposing a clean  $(1 \times 1)\text{Pt}(110)$  sample to nominally 0.4 langmuir of methanol at 100 K and then sequentially annealing to successively higher temperatures for 1 min, quenching, and recording an EELS spectrum.

All of the features shrink upon further annealing. The 2900  $\text{cm}^{-1}$  peak also shifts to 3050  $\text{cm}^{-1}$ . At 600 K, there are still distinct peaks at 600 and 1200  $\text{cm}^{-1}$ .

We have also done EELS measurements with  $\text{CD}_3\text{OD}$ . Figure 5 shows a series of EELS spectra taken by exposing a clean 100 K  $(1 \times 1)\text{Pt}(110)$  sample to 1.47 langmuirs of  $\text{CD}_3\text{OD}$  and then sequentially heating to successively higher temperatures. At 100 K we observe peaks at 560, 1000, 1100, 2080, 2230, and 2430  $\text{cm}^{-1}$ . The peak at 2500  $\text{cm}^{-1}$  disappears upon annealing to 200 K, but there is little other change in the spectrum. The 550  $\text{cm}^{-1}$  peak grows upon further annealing while all of the other peaks shrink. However, the 1100  $\text{cm}^{-1}$  peak is still evident even at 600 K.

AES measurements have also been done during experiments like those above. When a clean 100 K  $(1 \times 1)\text{Pt}(110)$  sample is saturated with methanol and then heated to 140 K, about  $0.32 \times 10^{15}$  carbon and oxygen atoms/ $\text{cm}^2$  are left on the surface. The carbon AES signal does not change upon further heating to 200 K. However, the oxygen signal is attenuated by a factor of 5–10. About half of the carbon leaves between 200 and 300 K. The remainder of the carbon remains on the surface to high temperatures.

#### Discussion

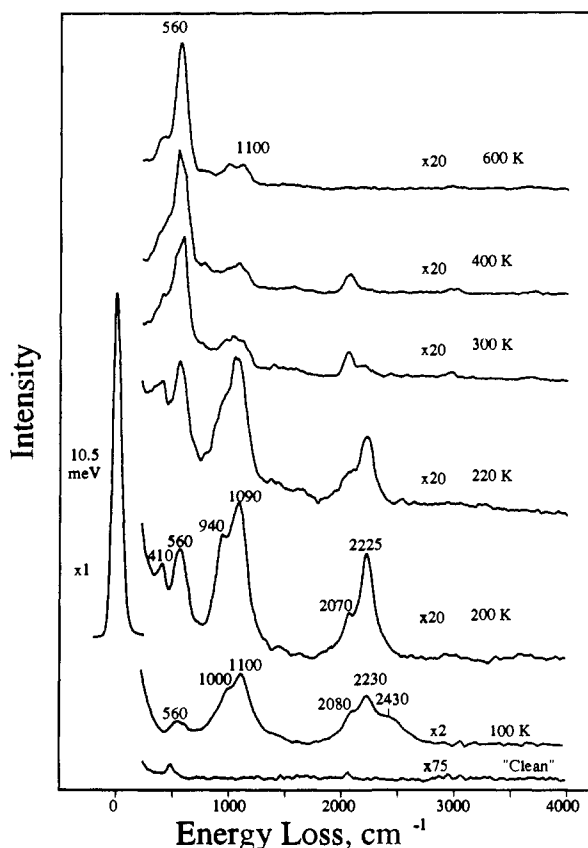
The results above show that methanol decomposition on  $(1 \times 1)\text{Pt}(110)$  is quite different than methanol decomposition on all of the faces of platinum examined previously.<sup>3–5,22,29</sup> While CO and hydrogen are the main products of methanol decomposition on all of the faces of platinum considered previously, little CO desorption is seen from  $(1 \times 1)\text{Pt}(110)$ . Instead the main decomposition products are water, methane, and hydrogen. AES also suggests that  $(1 \times 1)\text{Pt}(110)$  shows unique behavior. On other faces of platinum, the carbon and oxygen peaks decrease simultaneously upon heating.<sup>12</sup> However, on  $(1 \times 1)\text{Pt}(110)$ , the oxygen peak

**Table I.** Comparison of the Peak Positions in the EELS Spectrum of About  $2 \times 10^{14}$  molecules/cm<sup>2</sup> of Methanol Adsorbed on a 95 K (1×1)Pt(110) Sample to the Peak Positions in Previous EELS Spectra of Molecularly Adsorbed Methanol

assignment	CH <sub>3</sub> OH on (1×1)Pt(110)	CH <sub>3</sub> OH on (2×1)Pt(110) <sup>7</sup>	CH <sub>3</sub> OH on Pt(111) <sup>5</sup>	CH <sub>3</sub> OH liquid <sup>13</sup>	CH <sub>3</sub> OH vitreous solid <sup>13</sup>	CH <sub>3</sub> OH crystals <sup>13</sup>
O-H out-of-plane bend	740	760	680	655	730	790
C-O stretch	1060	1050	970	1029	1032	1029
CH <sub>3</sub> rock	1135	1135	-	1114	1124	1142
CH <sub>3</sub> bend	1470	1460	1430	1455	1452	1455
CH stretch	2960	2960	2930	2822, 2934	2928, 2951	2829, 2955
OH stretch	3275	3330	3320	3327	3235	3284, 3187
unassigned (overtone)		2590				

assignment	CD <sub>3</sub> OD on (1×1)Pt(110)	CD <sub>3</sub> OD on (2×1)Pt(110) <sup>7</sup>	CD <sub>3</sub> OD liquid <sup>13</sup>	CD <sub>3</sub> OD vitreous solid <sup>13</sup>	CD <sub>3</sub> OD crystals <sup>13</sup>
O-D out-of-plane bend	560	560	483	533	578, 495
C-O stretch	1000	990	979	975	968
CD <sub>3</sub> rock		780	818	831	862
CD <sub>3</sub> bend	1100	1100	1097	1100	1080
CD stretch	2080, 2230	2070, 2235	2082, 2225, 2250	2075, 2213	2075, 2212
OD stretch	2430	2410	2474	2384	2361, 2432

**Figure 5.** A series of EELS spectra taken by exposing a clean (1×1)-Pt(110) sample to nominally 1.47 langmuirs of CD<sub>3</sub>OD at 100 K and then sequentially annealing the sample to successively higher temperatures for 1 min, quenching, and recording an EELS spectrum.

virtually disappears upon heating to 200 K while the carbon peak is only weakly affected. Hence, it is clear that (1×1)Pt(110) shows unique properties for methanol desorption.

We can speculate about the mechanism of methanol decomposition on (1×1)Pt(110). Table I compares the peak positions in our low-coverage 100 K EELS spectra to those of molecularly adsorbed methanol. Notice the excellent agreement. Therefore, it seems that the methanol adsorbs molecularly at 100 K on (1×1)Pt(110).

There are subtle changes in the EELS spectra upon heating to 140 K. The 3300 cm<sup>-1</sup> peak shifts closer to the gas-phase OH

stretching frequency, and the 1100 cm<sup>-1</sup> mode is enhanced. Simultaneously, methanol desorption is seen in TPD. However, the EELS spectrum of the adsorbed layer still matches the EELS spectrum of molecularly adsorbed methanol. Therefore, it seems that there is still molecular methanol on the surface at 140 K.

At moderate coverages, some of that methanol desorbs between 140 and 190 K. However, at higher coverages, the tail in the methanol desorption peak between 140 and 190 K is attenuated. We still detect molecular methanol on the surface at 140 K with EELS. However, evidently the residual methanol reacts before it desorbs.

Water is the first decomposition product. The water desorbs in a broad peak extending up to 200 K. Simultaneously, oxygen disappears from the AES spectrum. The OH stretching modes at 740 and 3275 cm<sup>-1</sup> disappear from the EELS spectrum, and there is no evidence for the growth of an intense oxygen-platinum stretch at 350 cm<sup>-1</sup> like the one commonly observed when methoxy forms on other faces of platinum.<sup>5,12</sup> There still are modes around 2990 cm<sup>-1</sup>, suggesting that there are still CH bonds in the species on the surface. However, there is no evidence for any oxygen-containing species, except for a trace of CO. As a result, we conclude that the C-O bonds in the chemisorbed methanol break between 140 and 200 K, and the water product desorbs. EELS indicates that, at 200 K, the surface is covered mainly with CH<sub>x</sub> groups and/or possibly some other hydrocarbons.

The nature of the CH<sub>x</sub> layer is not completely clear from the data. The layer has the average stoichiometry of CH<sub>2</sub>. However, it is unclear whether there are just CH<sub>2</sub> groups on the surface or some mixture of species. Table II compares the peak positions in our 200 K EELS spectra of the EELS spectra of CH<sub>x</sub> species on other faces of transition metals. All of the spectra are very similar. The only major difference is that one expects a peak at about 1050–1100 cm<sup>-1</sup> with a CH<sub>2</sub> group and a peak at about 1120 cm<sup>-1</sup> with a CH<sub>3</sub> group. There appear to be several peaks between 1000 and 1100 cm<sup>-1</sup> in the 200 K spectrum in Figure 4, which suggests that there may be both CH<sub>2</sub> and CH<sub>3</sub> groups on the surface at 200 K.

The TPD data are consistent with this view. Notice that a significant CH<sub>2</sub>D<sub>2</sub> peak is seen when methanol and deuterium are coadsorbed. Roop et al.<sup>16</sup> found that little CH<sub>2</sub>D<sub>2</sub> is formed when CH<sub>3</sub>, CD<sub>3</sub>, and H are coadsorbed. Thus, the CH<sub>2</sub>D<sub>2</sub> in Figure 3 must come from a reaction between adsorbed CH<sub>2</sub> groups and adsorbed deuterium, implying that CH<sub>2</sub> groups are present on the surface at 200 K.

The evidence for adsorbed CH<sub>3</sub> groups is less obvious. However, the observation of CH<sub>2</sub>D<sub>2</sub> implies that the CH<sub>2</sub> groups can be

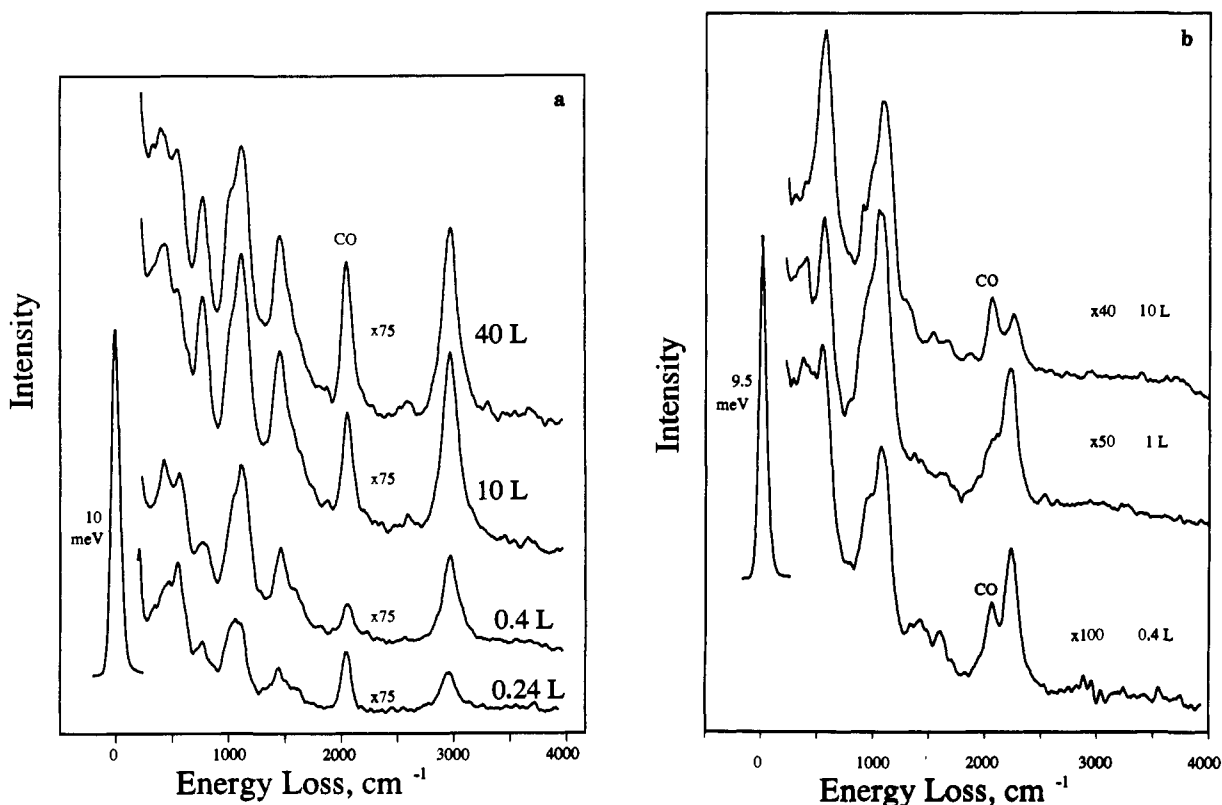
(13) Falk, M.; Whalley, E. *J. Chem. Phys.* **1961**, *34*, 1554.(14) McBreen, P. H.; Erley, W.; Ibach, H. *Surf. Sci.* **1984**, *148*, 292.(15) George, P. M.; Avery, N. R.; Weinberg, W. H.; Tebbe, F. N. *J. Am. Chem. Soc.* **1983**, *105*, 1393.(16) Roop, B.; Lloyd, K. G.; Costello, S. A.; Campion, A.; White, J. M. *J. Chem. Phys.* **1989**, *91*, 5103.(17) Demuth, J. E.; Ibach, H. *Surf. Sci.* **1978**, *78*, L238.(18) Stenhagen, E.; Abrahamsson, S.; McLafferty, F. W. *Atlas of Mass Spectral Data*; Wiley: New York, 1969; Vol. 1, p 2.(19) Davis, J. L.; Barteau, M. A. *Surf. Sci.* **1987**, *187*, 387.

**Table II.** Comparison of the Peak Positions in the EELS Spectrum Taken by Adsorbing Methanol onto a 100 K (1×1)Pt(100) Sample and Then Annealing to 200 K to the Peak Positions in Previous EELS Spectra of Adsorbed CH<sub>x</sub> Species

assignment	CH <sub>3</sub> OH on (1×1)Pt(110) annealed to 200 K	CH <sub>2</sub> ad from CH <sub>2</sub> CO on Fe(110) <sup>14</sup>	CH <sub>2</sub> ad from CH <sub>2</sub> N <sub>2</sub> on Ru(001) <sup>15</sup>	CH <sub>3</sub> ad from CH <sub>3</sub> Cl on Pt(111) <sup>16</sup>	CH <sub>3</sub> ad from CH <sub>3</sub> Br on Pt(111) <sup>16</sup>	CH from C <sub>2</sub> H <sub>2</sub> on Ni(111) <sup>17</sup>
metal-carbon stretch	430, 570	650	550, 650	516	495	NR
CH deformation	760			784	820	780
CH <sub>x</sub> rock	760	790	775	985		
CH <sub>x</sub> twist	-	930	900			
CH <sub>x</sub> wag	1030, 1130	1020	1135	1174	1180	
CH <sub>x</sub> bend	1460, 1560	1430	1450	1390	1410	
CH <sub>x</sub> stretch	2980	2970	2980	2977	2950, 2770	2980

assignment	CD <sub>3</sub> OD on (1×1)Pt(110) annealed to 200 K	CD <sub>2</sub> from CD <sub>2</sub> N <sub>2</sub> on Ru(001) <sup>15</sup>	CD <sub>3</sub> Cl <sup>27</sup>	CD <sub>3</sub> from CD <sub>3</sub> ion Pt(111) <sup>28</sup>	CD from C <sub>2</sub> D <sub>2</sub> on Ni(111) <sup>17</sup>
metal-carbon stretch	560	625		530	550
CD <sub>x</sub> rock	-		767		
CD <sub>x</sub> twist	-	680		855	
CD <sub>x</sub> wag	800	840		890	
CD <sub>x</sub> bend	940, 1090	1210	1029, 1060	1150	940
CD <sub>x</sub> stretch	2070, 2225	2210	2160, 2283	2080, 2235	2160

**Figure 6.** A series of EELS spectra taken by exposing a clean (1×1)Pt(110) sample to various amounts of (a) CH<sub>3</sub>OH, (b) CD<sub>3</sub>OD and then annealing to 220 K.

hydrogenated to methane. It is difficult to find a reasonable pathway to go from CH<sub>2</sub>ad and two H<sub>ad</sub>'s to methane, which does not involve the formation of a CH<sub>3</sub>ad group. Thus, is it not unreasonable that CH<sub>3</sub>ad's would form. Neither TPD nor EELS is completely conclusive. However, our interpretation of the data is that there is a mixture of CH<sub>2</sub> and CH<sub>3</sub> groups on the surface at 200 K.

TPD shows that some of the CH<sub>x</sub> groups are hydrogenated to methane at 240 K. However, some fall apart to yield hydrogen and carbon. The carbon is not simply atomic carbon however. Notice that there are two peaks in the EELS spectrum at 600 K, at 500 and 1100 cm<sup>-1</sup>. A 500 cm<sup>-1</sup> peak is normally associated with a platinum-carbon stretch. However, no one has previously observed a carbon-platinum stretch at 1100 cm<sup>-1</sup>. Yet nothing but carbon is left on the surface at 600 K; all of the hydrogen has desorbed. In previous work,<sup>20</sup> carbon-carbon stretching bands

have been observed at 1100 cm<sup>-1</sup> during ethylene decomposition on Pt(100). Thus, it seems that carbon-carbon bonds are forming during methanol decomposition on (1×1)Pt(110).

In fact, there is evidence that carbon-carbon bonds actually start to form at 220 K. Figure 6 shows a series of EELS spectra taken by exposing a clean (1×1)Pt(110) surface to various amounts of methanol at 220 K. At low exposures, the peak positions are the same as in the 200 K spectrum in Figure 4. However, in addition, there is an extra shoulder at about 1040 cm<sup>-1</sup>. At higher exposures, the 1100 cm<sup>-1</sup> peak broadens in a way which suggests that there may be a second shoulder in the EELS

(20) Hatzikos, G. H.; Masel, R. I. *Surf. Sci.* **1987**, *185*, 479.(21) Steiniger, H.; Ibach, H.; Leywald, S. *Surf. Sci.* **1982**, *117*, 685.(22) Attard, G. A.; Chibane, K.; Ebert, H. D.; Parsons, R. *Surf. Sci.* **1989**, *224*, 311.

**Table III.** Comparison of the Peak Positions in the EELS Spectrum of Methanol Adsorbed onto a 220 K (1×1)Pt(110) Sample to the Peak Positions in Previous EELS Spectra of Adsorbed Ethylene

assignment	0.4 langmuir of methanol on 220 K (1×1)Pt(110)	10 langmuirs of methanol on 220 K (1×1)Pt(110)	di- $\sigma$ -ethylene on (2×1)Pt(110) <sup>8</sup>	$\pi$ -bound ethylene on (1×1)Pt(110) <sup>9</sup>	di- $\sigma$ -ethylene on Pt(111) <sup>21</sup>	Zeise's salt <sup>25</sup>	C <sub>2</sub> H <sub>4</sub> Br <sub>2</sub> gauge <sup>26</sup>
M-C stretch	450, 570	440, 570	475	410	470, 560	369	
CH <sub>2</sub> rock	NR	630	670	670	660	721	898
CH <sub>2</sub> twist	770	770	805	-	790	-	1104
CH <sub>2</sub> wag	930	NR	960	950	980	975	1278
CH <sub>3</sub> rock	1120	1120					
C-C stretch	1040	1040, 1220	1020	1210	1050	1243	1019
CH <sub>2</sub> bend	1465, 1580	1460	1430	1400, 1560	1430	1416, 1515	1420
CH <sub>2</sub> stretch	2960	2977	2950	2960, 3060	2920	3013, 3079	2953, 3000

assignment	0.4 langmuir of CD <sub>3</sub> OD on 220 K (1×1)Pt(110)	10 langmuirs of CD <sub>3</sub> OD on 220 K (1×1)Pt(110)	di- $\sigma$ -C <sub>2</sub> D <sub>4</sub> on (2×1)Pt(110) <sup>8</sup>	$\pi$ -bound C <sub>2</sub> D <sub>4</sub> on (1×1)Pt(110) <sup>9</sup>	di- $\sigma$ -C <sub>2</sub> D <sub>4</sub> on Pt(111) <sup>21</sup>	D <sub>4</sub> Zeise's salt <sup>25</sup>	C <sub>2</sub> D <sub>4</sub> Br <sub>2</sub> gauge
M-C stretch	420		480	430	450		
CD <sub>2</sub> rock						525	712
CD <sub>2</sub> twist	580	500	590		600		791
CD <sub>2</sub> wag			713	709	740	757	947
C-C stretch	930	930, 1300	940	1330	900 sh	1353	1014
CD <sub>2</sub> bend	1100	1100	1145	966	1150	962, 1059	1141
CD <sub>2</sub> stretch	2260	2260	2130, 2220	2225, 2300	2150, 2250	2193, 2332	2174, 2271

spectrum at about 1220 cm<sup>-1</sup>. There is also a corresponding stretch at 1300 cm<sup>-1</sup> in the spectrum of CD<sub>3</sub>OD which is well-resolved. Thus, it appears that some new species are forming at high coverages at 220 K.

We propose that this species is some sort of hydrocarbon since we do not see significant oxygen in the layer with AES at 220 K. Table III compares the peak positions in the spectra in Figure 6 to those of previous investigators. Notice there is excellent agreement between the peak positions in the spectra in Figure 6 and those of adsorbed ethylene, suggesting the possibility that some hydrocarbon species are forming during methanol decomposition on (1×1)Pt(110) at 220 K. A detailed comparison of the peak intensities in Figure 6 and the ethylene spectra of Yagasaki et al.<sup>6</sup> shows that there are significant differences in the peak intensities in Figure 6 and the peak intensities in the spectra of adsorbed ethylene. Also the evolution of our high-coverage spectra with heating is different than that observed during ethylene decomposition on (1×1)Pt(110). Hence, we do think we are forming ethylene at 220 K. However, there are clearly carbon-carbon bonds at high temperatures, and the 220 K EELS spectra are as expected if some sort of hydrocarbon species formed. Thus, it appears that there may be some conversion of methanol to hydrocarbon species on (1×1)Pt(110) at temperatures as low as 220 K.

Admittedly, this is not a surprising result. In previous work, Berlowitz et al.<sup>23</sup> deposited CH<sub>2</sub> groups (from diazomethane) on Pt(111) and found that ethylene formed upon heating. The same process has been observed during ketene decomposition on Pt(111) by Mitchell et al.<sup>24</sup> Thus, it is not surprising that the CH<sub>x</sub> groups, which are seen on the (1×1)Pt(110) surface at 200 K, react to form hydrocarbons upon heating. We observe different hydrocarbons than were seen with ketene or diazomethane, however.

Before we close, we did want to compare our results to what is known about methanol decomposition on other faces of group VIII metals. The results here show that methanol decomposition on (1×1)Pt(110) is quite different than methanol decomposition on other faces of platinum or on other faces of group VIII metals. On (1×1)Pt(110), the methanol decomposes to yield methane,

water, and some mixture adsorbed of C<sub>x</sub>H<sub>y</sub> groups. In contrast, no water or methane formation was observed by Sexton,<sup>5</sup> Attard,<sup>22</sup> Gibson,<sup>29</sup> or Wang<sup>7,12</sup> during methanol decomposition on other faces of platinum. In particular, when we change our sample preparation procedures to produce a (2×1) reconstruction, no formation of water or methane is detected. Little CO formation is observed during methanol decomposition on (1×1)Pt(110). In contrast, CO was always<sup>19</sup> the major carbon-containing product during methanol decomposition on the faces of group VIII metals examined previously. There also is significant carbon deposition during our methanol decomposition on (1×1)Pt(110). Much less carbon deposition is seen on other group VIII metals. In particular on (2×1)Pt(110), no buildup of carbon is detected<sup>12</sup> with AES or EELS under conditions identical to those used here. We also observe EELS peaks at about 2900 cm<sup>-1</sup>, suggestive of CH modes at temperatures up to 400 K. By comparison, no CH modes are observed above 230 K on (2×1)Pt(110)<sup>12</sup> or on Pt(111).<sup>5</sup> Thus, it seems that the decomposition of methanol on (1×1)Pt(110) is far different than methanol decomposition on the faces of group VIII metals examined previously.

Our results on (1×1)Pt(110) do have some correspondence to the previous results of Levis et al.<sup>1,3</sup> We find that, on (1×1)Pt(110), the adsorbed methanol undergoes a C-O bond scission process to yield water and a mixture of CH<sub>x</sub> groups. Levis et al. observe the same chemistry on Pt(111). Of course, our results are specific to the (1×1) reconstruction of Pt(110). If we change our sample preparation procedures to get a (2×1) reconstruction, we do not observe formation of water or CH<sub>x</sub> groups. Instead, the reaction follows the pathway outlined in Guo et al., i.e., decomposition to CO and H<sub>2</sub>. Still, our results do show that the chemistry postulated by Levis et al. can occur on the appropriate sites on platinum catalysts. The question remains whether the reaction will occur on a perfect Pt(111) surface.

## Conclusion

In summary then, the results here show that methanol adsorbs molecularly on (1×1)Pt(110). Upon heating, the C-O bond in the methanol breaks to yield water and a mixture of CH<sub>x</sub> intermediates. The CH<sub>x</sub> groups then further react to form methane, hydrogen, adsorbed carbon, and some as yet unidentified hydrocarbon species. The observation of water and CH<sub>x</sub> intermediates is consistent with the previous observations by Levis et al.<sup>1,3</sup> However, the measurements are specific to the (1×1) reconstruction of Pt(110). In previous work,<sup>12</sup> we did not detect formation of water or CH<sub>x</sub> species when we changed our sample

(23) Berlowitz, P.; Yang, B. L.; Butt, J. B.; Kung, H. H. *Surf. Sci.* **1985**, *159*, 540.

(24) Radloff, P. L.; Mitchell, G. E.; Greenleaf, C. M.; White, J. M. *Surf. Sci.* **1987**, *183*, 377.

(25) Hiraishi, J. *Spectrochim. Acta, Part A* **1969**, *25*, 749.

(26) Neu, J. T.; Gwinn, W. D. *J. Chem. Phys.* **1950**, *18*, 1642.

(27) Shimanouchi, T. *Tables of Molecular Vibrational Frequencies*, NSRDS-NBS 39, National Bureau of Standards, 1972.

(28) Henderson, M. A.; Mitchell, G. E.; White, J. M. *Surf. Sci.* **1987**, *184*, L325.

(29) Gibson, K. D.; Dubois, L. H. *Surf. Sci.* **1990**, *223*, 59.

preparation procedure to produce the (2×1) reconstruction of Pt(110). Hence, our conclusion is that the rate of CO bond scission varies very strongly with surface structure and the details of the sample preparation procedure. This may explain why bond scission was observed by Levis et al.<sup>1,3</sup> and Madix<sup>4</sup> but not by Guo et al.,<sup>2</sup> Sexton,<sup>5</sup> or Gibson.<sup>29</sup>

**Acknowledgment.** This work was supported by the National

Science Foundation under Grant CTS 89-22282 and by Amoco Oil Co. and Shell USA. Sample preparation was done using the facilities of the University of Illinois Center for Microanalysis of Materials, which is supported as a national facility, under National Science Foundation Grant DMR 89-20538. Equipment was provided by NSF Grants CPE 83-51648 and CBT 87-04667.

**Registry No.** CH<sub>3</sub>OH, 67-56-1; Pt, 7440-06-4.

## Communications to the Editor

### Synthesis of the First Distillable $\alpha$ -Boranyldiazomethane. Direct Evidence of Lithioboranyldiazomethane-Lithioboranylisodiazomethane [( $>$ BCNN<sup>-</sup>,Li<sup>+</sup>)-( $>$ BNNC<sup>-</sup>,Li<sup>+</sup>)] Rearrangement

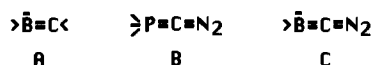
Marie-Pierre Arthur, Antoine Baccaredo, and Guy Bertrand\*

Laboratoire de Chimie de Coordination du CNRS  
205 route de Narbonne, 31077 Toulouse Cédex, France

Received January 15, 1991

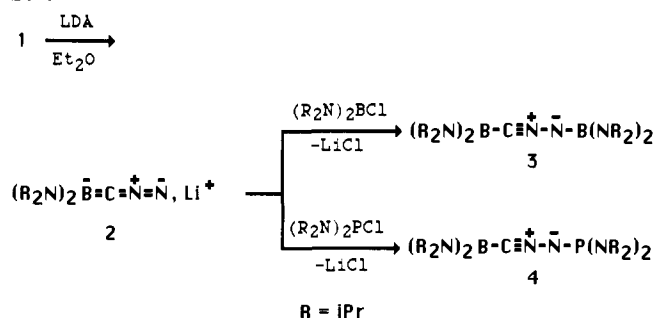
Revised Manuscript Received May 15, 1991

Main group element substituted diazo compounds have been widely studied<sup>1</sup> except in the boron series. Indeed, only two examples of C-substituted  $\alpha$ -boranyldiazomethanes, characterized by IR in solution, have been reported so far.<sup>2</sup> The lack of examples of this class of compounds is probably due to the ability of Lewis acids to catalyze the decomposition of diazo derivatives.<sup>1</sup> Boron-stabilized carbanions A have been widely used in organic synthesis, and X-ray diffraction studies have shown that they present a boron-carbon double bond character.<sup>3</sup> We have recently shown that (diazomethylene)phosphoranes B are stable at room temperature and that they are diazocarbene (:C=N<sub>2</sub>) or naked carbon atom generators, as well as powerful building blocks in heterocyclic chemistry.<sup>4</sup> Thus it was of interest to try preparing a new type of cumulene C, featuring both a diazo group and a borataalkene moiety.

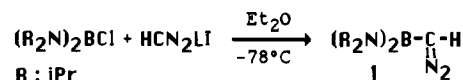


In the hope of obtaining a stable C-unsubstituted  $\alpha$ -boranyldiazomethane, and to further produce a carbanion  $\alpha$  to boron, we chose to synthesize [bis(diisopropylamino)boranyl]diazomethane (1). The attachment to boron of heteroatoms that are capable of  $\pi$ -donation is of primary importance to decrease the Lewis acidity and to prevent, in the second step, attack on the boron atom itself by the base, which would lead to a coordinatively saturated borate complex. Compound 1 is easily available by addition of a stoichiometric amount of bis(diisopropylamino)-

#### Scheme I



chloroborane<sup>5</sup> to an ethereal solution of the lithium salt of diazomethane,<sup>6</sup> at -78 °C.



Diazoborane 1 is thermally stable and was obtained in 54% yield as a yellow oil after distillation (bp 70–74 °C/10<sup>-1</sup> mmHg). The spectroscopic data<sup>7</sup> allowed exclusion of all its possible structural isomers; of particular interest were a strong IR absorption at 2071 cm<sup>-1</sup> ( $\nu$  CN<sub>2</sub>), a signal at 36.5 ppm ( $J_{\text{CH}} = 169.5$  Hz) broadened by the proximity of boron in the <sup>13</sup>C NMR spectrum, a signal at +34.5 in the <sup>11</sup>B NMR spectrum, and two signals at -114.2 ( $\nu_{1/2} = 80$  Hz, CNN) and -44.6 ( $\nu_{1/2} = 430$  Hz, CNN) in the <sup>14</sup>N NMR spectrum, in the range expected for the diazo nitrogens.<sup>8</sup>

An ethereal solution of diazo 1 was treated, at -78 °C, with a slight excess of lithium diisopropylamide (LDA). After stirring for a few hours at room temperature, the sharp IR absorption due to the diazo 1 was replaced by a broad band at 2080 cm<sup>-1</sup>, and a new broad signal appeared at 26 ppm in the <sup>11</sup>B NMR spectrum. Addition of bis(diisopropylamino)chloroborane and bis(diisopropylamino)chlorophosphane to this ethereal solution of 2 af-

(5) Higashi, J.; Eastman, A. D.; Parry, R. W. *Inorg. Chem.* **1982**, *21*, 716.

(6) The lithium salt of diazomethane was prepared by a modification of the published procedure: (a) Müller, E.; Ludsteck, D. *Chem. Ber.* **1954**, *87*, 1887. (b) Müller, E.; Rundel, W. *Chem. Ber.* **1955**, *88*, 917; **1957**, *90*, 1299, 1302, 2673.

(7) All isolated compounds afforded satisfactory elemental analysis. Selected physical data are the following: 1: <sup>1</sup>H NMR (C<sub>7</sub>D<sub>8</sub>, 298 K) 1.05 (d,  $J_{\text{HH}} = 6.6$  Hz, 24 H, CH<sub>3</sub>), 3.17 (s, 1 H, CN<sub>2</sub>H), 3.47 (sept,  $J_{\text{HH}} = 6.6$  Hz, 4 H, CH); <sup>13</sup>C NMR (C<sub>7</sub>D<sub>8</sub>, 223 K) 22.90 (s, CH<sub>3</sub>), 36.51 (s, CN<sub>2</sub>), 45.89 (s, CH). 3: yellow oil, bp 110–120 °C/10<sup>-3</sup> mmHg; <sup>11</sup>B NMR (C<sub>7</sub>D<sub>8</sub>, 363 K) +23.5, +27.8; <sup>13</sup>C NMR (C<sub>7</sub>D<sub>8</sub>, 223 K) 65.8 (br s, CNN); <sup>14</sup>N NMR (C<sub>7</sub>D<sub>8</sub>, 348 K) -186.4 ( $\nu_{1/2} = 140$  Hz, CNN), -285 ( $\nu_{1/2} = 1300$  Hz, NR<sub>2</sub>); IR (ether) 2160 cm<sup>-1</sup>. 4: yellow oil, bp 105–110 °C/10<sup>-3</sup> mmHg; <sup>11</sup>B NMR (C<sub>6</sub>D<sub>6</sub>) +22; <sup>31</sup>P NMR (C<sub>6</sub>D<sub>6</sub>) +96.6; <sup>13</sup>C NMR (C<sub>6</sub>D<sub>6</sub>) 67.0 (br s, CNN); <sup>14</sup>N NMR (C<sub>6</sub>D<sub>6</sub>, 298 K) -184.4 ( $\nu_{1/2} = 220$  Hz, CNN), -320 ( $\nu_{1/2} = 1500$  Hz, NR<sub>2</sub>); IR (ether) 2145 cm<sup>-1</sup>. 6: yellow oil, bp 110–115 °C/0.2 mmHg; <sup>11</sup>B NMR (CDCl<sub>3</sub>) +29; <sup>31</sup>P NMR (CDCl<sub>3</sub>) +45.1; <sup>13</sup>C NMR (C<sub>6</sub>D<sub>6</sub>) 61.87 (d,  $J_{\text{PC}} = 48.3$  Hz, CNN); IR (CDCl<sub>3</sub>) 2113 cm<sup>-1</sup>.

(8) The <sup>14</sup>N NMR signals of diazo compounds are in the range -110 to -125 for CNN and -20 to -74 for CNN, while for nitrilimines only one nitrogen (CNN) is observable between -170 and -215: Horchler v. Locquenghien, K.; Reau, R.; Bertrand, G., submitted for publication.

(1) For reviews, see: (a) Patai, S. *The Chemistry of Diazonium and Diazo Groups*; Wiley: New York, 1978. (b) Regitz, M. *Diazoalkanes*; Georg Thieme Verlag: Stuttgart, 1977. (c) Regitz, M.; Maas, G. *Top. Curr. Chem.* **1981**, *97*, 71. (d) Regitz, M.; Maas, G. *Diazo Compounds, Properties and Synthesis*; Academic Press: Orlando, 1986.

(2) (a) Tapper, A.; Schmitz, T.; Paetzold, P. *Chem. Ber.* **1989**, *122*, 595. (b) Schöllkopf, U.; Banhidai, B.; Frasnelli, H.; Meyer, R.; Beckhaus, H. *Justus Liebig's Ann. Chem.* **1974**, 1767.

(3) (a) Wilson, J. W. *J. Organomet. Chem.* **1980**, *186*, 297. (b) Garad, M. V.; Pelter, A.; Singaram, B.; Wilson, J. W. *Tetrahedron Lett.* **1983**, *24*, 637. (c) Olmstead, M. M.; Power, P. P.; Weese, K. J.; Doedens, R. J. *J. Am. Chem. Soc.* **1987**, *109*, 2541. (d) Bartlett, R. A.; Power, P. P. *Organometallics* **1986**, *5*, 1916.

(4) Sotiropoulos, J. M.; Baccaredo, A.; Bertrand, G. *J. Am. Chem. Soc.* **1987**, *109*, 4711.